Journal of Energy

VOLUME 67 Number 1 | 2018 Special Issue

journal homepage: http://journalofenergy.com/

Martin Dadić
University of Zagreb
Faculty of Electrical Engineering and Computing / FER
Zagreb, Croatia, martin.dadic@fer.hr

Monika Sandelić
Aalborg University
Department of Energy Technology,
Aalborg, Denmark, msande16@student.aau.dk

Hrvoje Hegeduš
University of Zagreb
Faculty of Electrical Engineering and Computing / FER
Zagreb, Croatia, hrvoje.hegedus@fer.hr

Goran Petrović
University of Split
Faculty of Electrical Engineering, Mechanical Engineering and Naval Architecture
Split, Croatia, goran.petrovic@fesb.hr

A Circular Loop Time Constant Standard

Summary

A time constant standard, developed for the phase angle measurement of precision current shunts is developed and described, and its time constant has been determined. Based on a single circular loop placed in an air thermostat, its construction is very simple and it gives accurate results in the frequency band of interest, e.g. for frequencies between 50 Hz and 100 kHz. The influence of the shielding is calculated using numerical Finite Element Analysis (FEA). The thermostatic stability is analyzed, and the time-constant of the thermostat is determined using temperature measurement and Butterworth filtering. The power coefficient of the standard is determined, and limits of errors are discussed.

Key words: time constant standard, circular loop, phase angle measurment, thermostat, Finite Element Method (FEM)

Introduction

An increased interest in correct measurement of current over a wide frequency range is triggered by a widespread application of equipment like power converters, power electronics and nonlinear loads, which produce higher harmonics. Therefore, the phase angle reference is important for the determination of the phase angle errors of precision AC/DC shunts. Additionally, it is also needed in other applications like capacitor loss factor calibration. Classical designs of calculable resistors include Haddad, bifilar and folded loops [1,2]. In [3] a simple resistance standard with calculable time constant is described. In [4] a coaxial time constant standard for the determination of phase angle errors of current shunt is presented.

The main goal of this paper is to present a time constant standard for the determination of phase angle errors of current shunts, using a recently developed phase comparator based on a PXI NI 4461 system and LabView environment. While it is generally possible to match the parasitic inductance and capacitance to resistance of the standard in such a way that the time constant is as close as possible to zero [2],[3], it is decided, due to the computational flexibility of the LabView to digitally compensate the phase lag of the standard instead. This allows simpler design and easier manufacturing of the standard. The targeted frequency bandwidth of the standard is 50 Hz - 100 kHz.

Design of Circular Loop Standard

The standard is based on a single circular loop. If the diameter of the wire is chosen to be sufficiently small comparing to the skin depth, its inductance and resistance will be constant over the desired frequency bandwidth, and it is easily precisely calculated. In comparison to the bifilar and folded loops, the mutual inductance does not exist, as well as the proximity effect and the parasitic capacitance between loops. The main difference between the actual inductance and the inductance of the ideal circular loop is a small gap in the loop needed for the connection of the external cables. To cope with this effect, it is decided to measure the inductance using a precision LCR bridge instead of using the calculated inductance values. The loop is mounted in a massive passive aluminum thermostat, which serves in the same time as the electrostatic shield of the system and averages the ambient temperature changes. The equivalent circuit of the time constant standard is depicted in Fig. 1.

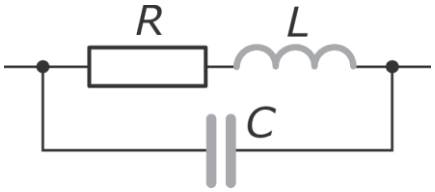

Figure 1. Equivalent circuit of the resistor

The resistance is, as well as the inductance constant over the frequency bandwidth of interest if the wire diameter is sufficiently small in comparison with the skin depth. The inductance will be, for the mounted loop in the electrically conductive thermostat, generally frequency dependent to the some level, which is investigated using the Finite Element Analysis (FEA). The capacitance *C* is defined by the capacitance of the cables, which was measured using a LCR bridge.

The time constant τ can be expressed approximately for most values of *R* and *C* as [3-5]

$$\tau = \frac{L}{R} - RC \tag{1}$$

with the phase angle of the standard

$$\varphi = 2\pi f \times \tau \tag{2}$$

The circular loop is wound using a manganin wire with the diameter 0.07 mm on a circular plastic former (Fig. 2). For the easier assembling, a circular gutter was machined in the former. The radius of the manganin loop (taking into account the gutter depth and the radius of the former) was fi-

nally 25.035 mm. The loop is connected with two coaxial cables Amphenol RG 223U, for the 4-wire connection in the external bridge circuit. The current cable is equipped with a N-type connector that matches our serial T-piece, while the sense (potential) cable is equipped with a BNC connector. The sleeve of the sense cable is connected to the shield (thermostat), thus forming the electrostatic shield and shunting the capacitance between the loop and the shield.

Figure 2. Former with the circular loop mounted on the top plate of the thermostat

Analytical Calculation of the Inductance

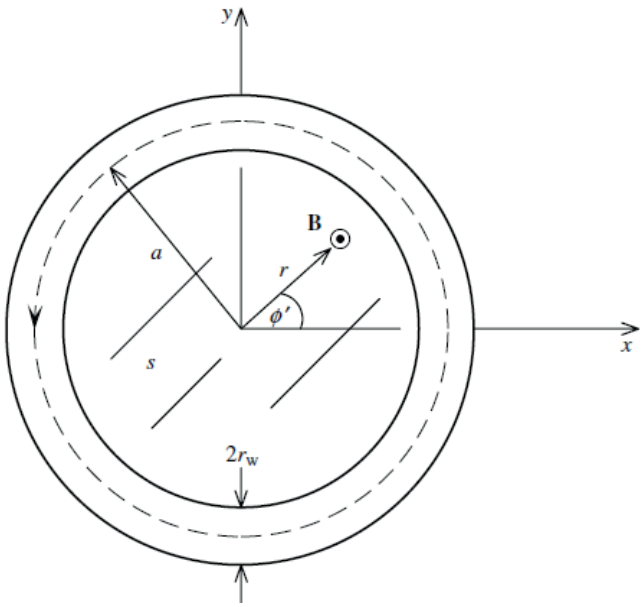

Figure 3. Model of the circular loop wire

The inductance of the circular loop (Fig. 3) can be calculated analytically approximately as [6]

$$L = \mu a\left(\ln\left(\frac{8a}{r_w}\right) - \frac{3}{2}\right) \tag{3}$$

Here, denotes radius of the loop, wire radius is andis permeability of the air. It is, further on, assumed that current is uniformly distributed over the entire cross section of the wire.

It should be pointed out that the expression (3) has certain inaccuracy based on the assumptions and approximations taken into account during deriving of the expression. The inaccuracy should be taken into account when using theoretically obtained values as reference points for further comparison with simulation and experimental results.

In Table I, dimensions of circular loop resistor and the obtained results of parasitic inductance are given.

Table I. Loop dimensions and analytically calculated inductance

a [mm]	r_w [mm]	L [μH]
25.035	0.035	0.225

Measurement of the Inductance

Figure 4. Inductance measurement

To determine the inductance L of the standard, the loop was initially wound using a copper wire with the same diameter, in the same manner as in [4]. In this way, the resistance is much smaller than the reactance of the loop, and at higher frequencies the inductance can be determined more precisely. The inductance was measured using a HP 4284A precision LCR meter using a custom-made test fixture (Fig. 4), open-short calibration and following settings: Integr: long, avg. 4, level 1 V and bias 0 V. In Table II, the measurement results are presented.

Table II. Measured inductance

f(kHz)	1	2	5	10	20
L(μH)	0.2240	0.2250	0.2240	0.2230	0.2240
R (Ω)	0.6164	0.6155	0.6156	0.6152	0.6152

f(kHz)	50	100	150	200	250
L(μH)	0.2240	0.2215	0.2207	0.2202	0.2198
R (Ω)	0.6158	0.6171	0.6171	0.6176	0.6173

f(kHz)	300	333.33	400	480	500
L(μH)	0.2195	0.2190	0.2191	0.2188	0.2187
R (Ω)	0.6185	0.6192	0.6196	0.6208	0.6210

From the Table II it may be concluded that the inductance and resistance does not change in the frequency band bellow 500 kHz. Above 500 kHz the results were inconsistent, which may be attributed to the test fixture, the parasitic capacitance or the calibration of the bridge.

Using all this information, the chosen inductance of the standard is the inductance measured in the middle of the measured frequency band, e.g. at 250 kHz, which is 0.2198 μH. The accuracy of the bridge is % of reading.

FEM Analysis

Conducting and magnetic shields are commonly used in prevention of undesired coupling among different coils and in reduction of the electromagnetic noise [7,8].

When a conducting shield is placed in the vicinity of the conductor, it changes magnetic field distribution produced by the current by open- circuiting the magnetic path. As a result, the eddy currents are induced in the shield and they couple with source current in a reverse manner. Therefore, the resultant magnetic field, in the vicinity of the source, is reduced. Consequently, the inductance of the circular loop wire inside the shield is reduced. Due to the fact that the effect of these phenomena is changing the inductance, its influence should be examined as to conclude if it can be neglected [9]. It was performed using the Finite Element Method (FEM) analysis.

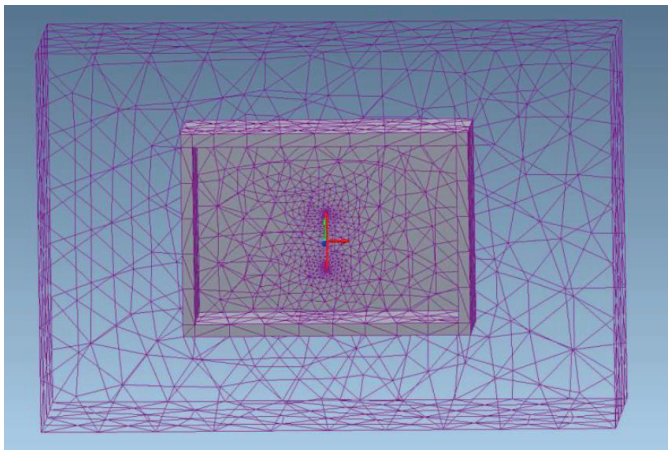

Figure 5. Mesh of finite elements

Simulations for the circular loop resistor were run in MagNet Infolytica software. The resistor is modeled according to the dimensions provided in Table I. Static and time harmonic simulations were performed. During static simulations, the maximum element size parameter has been adjusted in order to determine influence of the FEM grid construction on the obtained results. It was found that for the values of maximum element size equal to or smaller then 0.1 mm, the simulation results do not deviate much from theoretically obtained value. Therefore, it is decided that the maximum element size is set to 0.15 mm for further time harmonic simulations. In addition, it should be pointed out that duration of the simulation process is an important parameter in determination of the optimal maximum element size value. As for better and more accurate results, the grid should be constructed of greater number of small elements, which consequently, require longer processing time.

For the maximum element size equal to 0.15 mm, the calculated inductance using FEM was 0.24913 μH.

The simulation results describing the influence of the electrostatic shield on copper wire inductance is shown in Fig. 3. As it may be observed, inductance value is higher for the case without electrostatic shield. The simulated results correspond to expected values based on the theory.

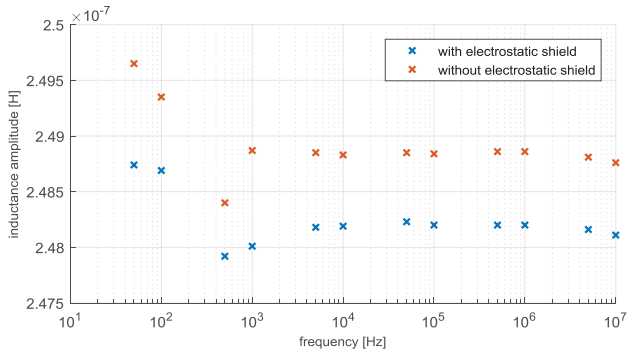

Figure 6. Change of inductance with the frequency for copper wire

The inductance values calculated using FEM follow the same trend with the frequency, with expected lower values for the shielded loop, due to the induced eddy currents in the shield (thermostat). The frequency dependence of the curve for the shielded case can be attributed to the skin effect, which influences the induced currents in the shield, and the errors in the simulations, which are inevitable. The biggest difference between shielded and un-shielded case in the calculated inductance (for the calculated set of frequencies) is at 50 Hz, and it is 0.3652 %. It should be added to the accuracy of the measurement of the inductance using the LCR bridge, since the measurements were performed without the shield. Fig. 6 also suggests the change of the inductance with the frequency (due to the errors in the simulations and the skin effect). The biggest difference for the shielded case relatively to the inductance calculated at 50 Hz (as the reference value) is at 500 Hz, and it equals 0.3284 %. In the conservative approach, it is also added to the overall accuracy of the measured inductance.

The calculated change of the resistance is 0.02 ppm at 100 kHz, using the same FEM model and the manganin wire (instead of copper).

Thermostat

Thermostatic stability is another characteristic that should be taken into consideration as it influences on resistance of the circular loop wire. The main reason why these effects are investigated experimentally is because they might have an influence on the resistor and its values when subjected to different working environments.

The measurement set-up was consisted of 8 NTC resistors (10 kΩ, Thermometrics MC65F103A) as the temperature sensors, connected to the digital multimeter DM3064. Two NTC resistors were placed out of the thermostat, 4 resistors were tight connected to the thick aluminum plates which form the air thermostat (within the thermostat). The last two resistors were placed in the air within the thermostat. The multimeter was connected to a PC computer, and the analysis and data acquisition process was performed using a LabView program developed for this purpose.

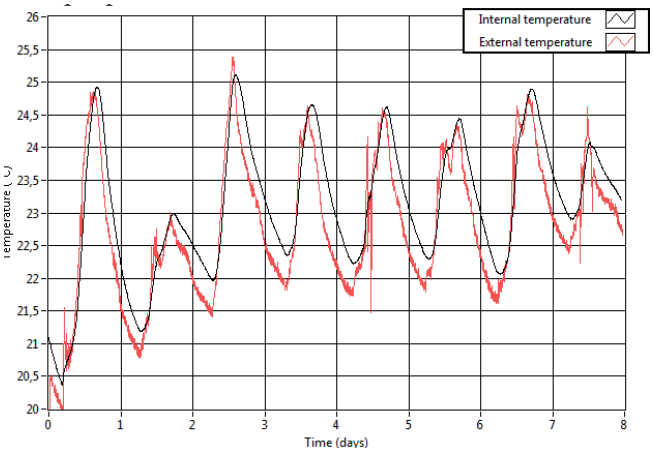

Figure 7. External and internal temperature of the thermostat during 8 days

Fig. 7 shows the changes of the internal temperature of the thermostat, compared to the ambient temperature. It is seen that the thermostat, due to its massive construction, efficiently cope with the transient, short-time variations in the ambient temperature, and that it introduces an expected delay in the global trend in the change of the temperature.

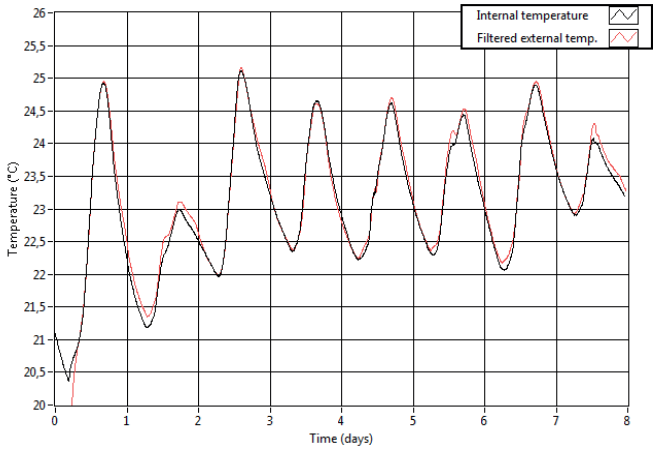

Figure 8. Filtered external vs. internal temperature of the thermostat

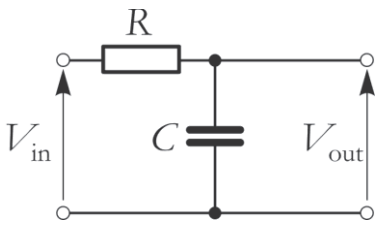

Figure 9. RC integrator circuit

The time-constant of the thermostat was estimated using the lumped heat-capacity approach [10]. The thermostat is as the thermal system consisted of the thermal capacitance and the thermal resistance. It exhibits filtering characteristics like an RC integrator circuit, depicted in Fig. 9. The frequency response (magnitude) of the RC integrator from Fig. 9 is

$$H_{RC}(\omega)=\frac{V_{out}}{V_{in}}=\frac{1/\omega C}{\sqrt{R^2+(1/\omega C)^2}}=\frac{1}{\sqrt{1+(\omega RC)^2}}=\frac{1}{\sqrt{1+(\omega/\omega_0)}} \quad (4)$$

Where C is the equivalent electric capacitance, R is equivalent electric resistance, ω denotes radian frequency and

$$\omega_0=\frac{1}{RC} \quad (5)$$

is – 3dB cutoff radian frequency of the integrator. It is forming a low-pass filter in the equivalent electrical network. Let's define the transfer function (magnitude) of a Butterworth filter of order n with the same cutoff radian frequency [11]:

$$H(\omega)=\frac{1}{\sqrt{1+\left(\frac{\omega}{\omega_0}\right)^{2n}}} \quad (6)$$

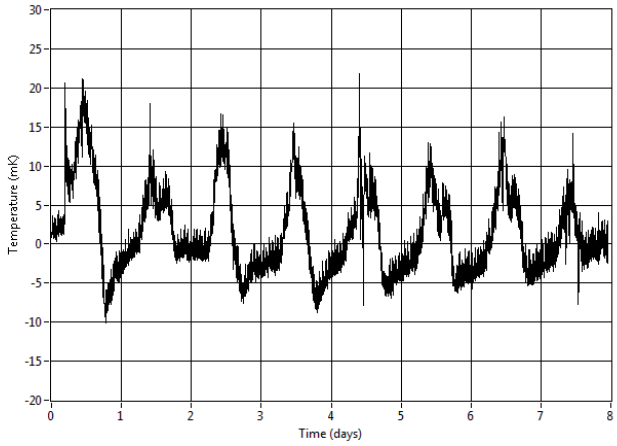

Figure 10. Difference between the temperature of the thermostat walls and the internal air temperature

For n=1 the transfer functions of the RC integrator and the Butterworth filter are the same. Therefore, to determine the cutoff frequency of the thermal system consisting the thermostat, the external temperature was filtered using a low-pass, first-order Butterworth filter. The filter was configured in LabView as the Infinite-Impulse-Response (IIR) digital filter. Its cutoff frequency was set in a manner that the low-pass filtered external temperature signal match in time the internal temperature (Fig. 8). The cutoff frequency was 28 μHz, which gives estimated time-constant of the system equal to 9.92 hours. The difference between the temperature of the thermostat walls and the internal air temperature is within 35 mK, and it is depicted in Fig. 10.

Measurement of Resistance and Capacitance

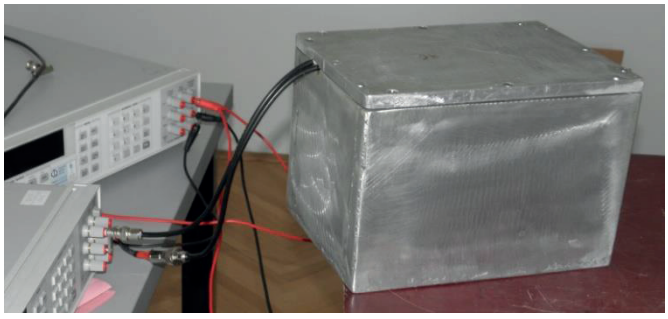

Figure 11. Assembled time constant standard during resistance measurement

The resistance was measured using an Agilent 3458A multimeter, with a 4-wire connection (Fig. 11). The measured DC resistance was R=20.16263 Ω, with the 2-year accuracy 20 ppm of reading + 10 ppm of range. For the 100 Ω range, the total accuracy is 1.4 mΩ, or 70 ppm of reading. The capacitance was measured using a Rohde&Schwarz (Hameg) HM8118 LCR bridge in 4-wire connection, using the Kelvin clamps. For the capacitance measurement, the cables were soldered in parallel (on the loop side) and the connectors were assembled, but the loop was not connected to the cables. Prior the measurement, the open-short calibration of the bridge was performed. The setting of the bridge was as follows: f=1 kHz, lev=1 V. The measured capacitance was C=96.091 pF. The accuracy of the measured capacitance is based on the equivalent impedance, which is 1.66 MΩ, and it equals 0.2104 %.

Power Coefficient

The power coefficient (PC) of the time constant standard influences its resistance, when it is used over wide range of currents. The power coefficient was characterized using a shunt of insignificant power coefficient (Method 4, [12]). At the Faculty of electrical engineering and computing, University of Zagreb, a set of cage type AC shunts has been produced [13, 14]. The PCs of shunts from this set, which have the rated currents less than 300 mA are insignificant. Therefore, the shunt with the rated current 100 mA was chosen as the reference standard (RSTD) for PC measurement. The circular loop resistance standard and RSTD were placed in series using a custom serial T-piece, while the current was supplied by a Rigol DP1116A DC single channel programmable power supply via a series resistor (1 kΩ for 10 mA current, and 100 Ω for 50 mA current). The current was monitored using a 61/2 digit digital multimeter (DMM) Rigol DM 3061, and the voltages across STD and circular loop resistance standard were measured using two 81/2 digit digital multimeter Agilent 3458A. The resistance ratio was measured for the currents equal to 10 mA and 50 mA, where the latter was chosen as the maximum current which still ensures that the voltage drop at the standard resistor fall within the 1 V range of DMM Agilent 3458A. The ratio of the voltages was measured after the time period that ensured that the loop resistor reached the constant resistance at each applied current. The determined PC is –3926 μΩ/Ω/W. The large PC is caused by the temperature coefficient of the manganin wire, together with a very small diameter of the wire. If the loop standard resistor is used with larger currents (50 mA or 70 mA), the correction of the resistance due to the power coefficient has to be included in the time-constant. If the applied current is kept at 10 mA, the change of the resistance due to the power coefficient (in the conservative approach, taking the PC as the constant) is –8 ppm, which can be included in the uncertainty, with a very small impact on the overall uncertainty. The resistance of the loop resistor, which was measured with DMM Agilent 3458A is, according to the data sheet of the manufacturer, measured at 1 mA current (at 100 Ω range) where the influence of the PC is insignificant.

Limits of Errors

Since the time constant is measured indirectly, the calculation of the safe limits of errors, as the maximum deviation of the device time constant from the true value is based on equations (1) and (2). The time constant of the standard is, using the measured values of R, L and C equal to 8.9639 ns. The limits of errors of the first term L/R in (1) are (0.3+0.3652+0.3284+0.007)%, which yields 1.0006 %. The second term in (2) is RC, and its limits of errors are (0.2104+0.007) %= 0.2174%.

For the equations including the difference as in (1), the overall safe limit of error is

$$G_{\%}=\pm\frac{|x_1G_{1\%}|+|x_2G_{2\%}|}{x_1-x_2} \quad (7)$$

where x_1 denotes first term (L/R) and x_2 denotes the second term (RC), while $G_{1\%}$ and $G_{2\%}$ are their accuracies [15].

For the measured R, L and C, the overall limit of errors is 1.264 % of the determined time constant or 113.30 ps.

This gives the limits of the phase angle error equal to 7.12 μrad or 0.00041° at 10 kHz, and the limits of the phase angle error equal to 71.19 μrad or 0.0041° at 100 kHz.

The minimum typical phase displacement of the Fluke A40B series precision current shunts (for shunts with nominal currents spanning from 1 mA to 100A) is below 0.006 ° at 10 kHz, and 0.060 ° at 100 kHz. At both frequencies, the limits of the phase angle errors of the time constant standard

is more than 10 times smaller of the expected measured phase angles, which makes the standard suitable for the determination of the phase angle displacements of such a type of the precision currents shunts.

Conclusions

A time constant standard, developed for the phase angle measurement of precision current shunts is developed and described, and its time constant has been determined. Based on a single circular loop, its construction is very simple and it gives accurate results in the frequency band of interest, e.g. for frequencies between 50 Hz and 100 kHz. Based on the power rating of 100 mW (in the air thermostat) and the DC resistance of the time constant standard, the maximum permissible current is 70 mA, which makes it suitable for the measurement of the phase angle error of shunts with the nominal current equal to 100 mA (and resistances typically equal to approximately 7 Ω). The correction of the resistance due to the power coefficient has to be taken into account. The time constant standard is also suitable for the measurement of the phase angle measurement of 10 mA shunts (with typical resistances equal to approximately 70 Ω), where the power rating is 2 mW. Using the step-up procedure [15] and the phase angle comparator, already developed at our laboratory [13], the phase angle displacement for the whole set of precision current shunts with nominal currents spanning from 1mA to 10 A can be determined.

Acknowledgment

This work was fully supported by Croatian Science Foundation under the project Metrological infrastructure for smart grid IP-2014-09-8826.

References

[1] D. Gibbings, “A design for resistors of calculable a.c./d.c. resistance ratio,” Proceedings of the Institution of Electrical Engineers, vol. 110, no. 2, pp. 335–347, February 1963.

[2] F. J. Wilkins and M. J. Swan, “Resistors having a calculable performance with frequency,” Proceedings of the Institution of Electrical Engineers, vol. 116, no. 2, pp. 318 - 324, 1969.

[3] S. Mašláň, M. Šíra; V. Nováková Zachovalová, J. Streit, „Simple resistance standard with calculable time constant,“ Conference on Precision Electromagnetic Measurements (CPEM 2016), Ottawa (ON), Canada, 2016, p. 1-2.

[4] Xianlin Pan, Jiangtao Zhang, Xuefeng Ma, Yang Gu, Wenfang Liu, Biao Wang, Zuliang Lu, and Deshi Zhang, »A Coaxial Time Constant Standard for the Determination of Phase Angle Errors of Current Shunts,« IEEE Trans. Instr. Meas, vol. 62, no. 1, January 2013, pp. 199-204.

[5] S. Svensson; K.-E. Rydler; V. Tarasso, »Improved Model and Phase-Angle Verification of Current Shunts for AC And Power Measurements,«

Conference on Precision Electromagnetic Measurements (CPEM 2004), London (UK), 2004, pp. 82-83,

[6] C. R. Paul, Inductance - Loop and Partial, John Wiley & Sons, 2010

[7] B.P. Kibble, G.H. Rayner, Coaxial AC Bridges, Adam Hilger, Bristol, 1984.

[8] H. W. Ott, Electromagnetic Compatibility Engineering, John Wiley & Sons, 2009

[9] L. Kefu, “Effect of a shield on the inductance of a conductor and its application to a compensated pulsed alternator,” in Fifth International Conference on Electrical Machines and Systems (ICEMS) , vol.2, 2001, pp. 1037-1041.

[10] J.P. Holman, Heat Transfer, McGraw-Hill, New York, 1997.

[11] Weinberg L. *Network Analysis and Synthesis*. McGraw-Hill;, New York, 1962.

[12] D. Deaver, N. Faulkner, Characterization of the Power Coefficient of AC and DC Current Shunts, 2010 NCSL International Workshop and Symposium, Providence, Rhode Island (USA)

[13] M. Dadić, P. Mostarac, R. Malarić, “Wiener Filtering for Real-Time DSP Compensation of Current Transformers over a Wide Frequency Range,” IEEE Transactions on Instrumentation and Measurement, vol. 66, no. 11, pp. 3023-3031, November 2017.

[14] Roman Malarić, Martin Dadić, Petar Mostarac:“D2.2. Report on designing, developing and testing current shunts“, Deliverable D.2.2. of Croatian Science Foundation project SMA-GRIMET, April 15th, 2016, 20 pp (in Croatian)

[15] V. Bego, Mjerenja u elektrotehnici, Tehnička knjiga, Zagreb, 1988.

[12] G. C. Bosco, M. Garcocz, K. Lind, U. Pogliano, G. Rietveld, V. Tarasso, B. Voljc, and V. N. Zachovalová, “Phase comparison of high current shunts up to 100 kHz,” IEEE Trans. Instrum. Meas., vol. 60, no. 7, pp. 2359–2365, Jul. 2011.